SDSS'Rio 2010 STABILITY AND DUCTILITY OF STEEL STRUCTURES
E. Batista, P. Vellasco, L. de Lima (Eds.)
Rio de Janeiro, Brazil, September 8 - 10, 2010

FIRE BEHAVIOR OF CONCRETE FILLED CIRCULAR HOLLOW SECTION COLUMNS WITH MASSIVE STEEL CORE

Martin Neuenschwander, Markus Knobloch and Mario Fontana

ETH Zürich, Institute of Structural Engineering –
Steel, Timber and Composite Structures, 8093 Zürich, Switzerland
e-mails: neuenschwander@ibk.baug.ethz.ch, knobloch@ibk.baug.ethz.ch, fontana@ibk.baug.ethz.ch

Keywords: Fire resistance; Steel-concrete composite; Concrete-filled steel CHS columns; Buckling

Abstract. *The paper analyses the structural fire behavior of centrically loaded concrete-filled steel CHS with a massive steel core. A numerical model for a geometrically and temperature-dependent materially nonlinear analysis of the imperfect structure is presented. A comprehensive numerical study shows the influence of the thermal expansion as well as the bonding behavior between steel and concrete on the structural fire behavior.*

1 INTRODUCTION

Concrete-filled circular hollow steel section columns (CHS) with a massive steel core have an attractive slender appearance due to their typical high slenderness ratio of the column. They can be used for heavily loaded columns and/or for minimizing the size of the column. Subjected to fire conditions the steel tube is directly exposed to the fire and heats up quickly. The concrete inside the tube slows down the heating of the steel core. At elevated temperatures the strength and stiffness of steel and concrete decreases. The reduced strength and stiffness have a marked influence on both the cross-sectional capacity and the slender column strength of steel concrete composite sections. The load-carrying behavior of concrete-filled CHS with massive steel cores at ambient temperatures is recently studied experimentally and numerically by Hanswille/Lippes [1]. Fire resistance tests of centrically and eccentrically loaded concrete-filled hollow steel section columns with both plain and reinforced concrete (without steel cores) were performed by [2-6], for example. The use of reinforced concrete improves the fire resistance significantly [7]. Numerical studies on the fire behavior of concrete-filled hollow steel section columns are presented in [8,9]. The fire behavior of concrete-filled CHS with massive steel core has not been comprehensively analyzed so far. Hence, it is necessary to obtain basic data on the structural behavior of these columns and to develop a fire design model.

2 NUMERICAL MODEL

2.1 Finite element method model

A finite element model was developed using ABAQUS/Standard, Rel. 6.8 to analyze the load-carrying behavior of concrete-filled hollow steel tube columns with massive steel cores. The columns were modeled with linear three-dimensional continuum elements with a reduced integration scheme (C3D8R elements of the ABAQUS element library) for the entire section. The longitudinal axis coincided with the x-direction and the cross-sectional plane with the yz-plane. The radial symmetry of the temperature fields and the circular shape of the cross section allowed modeling only one half of the column with the xz-plane being a symmetry plane. The overall initial geometric imperfection was assumed to have a sinusoidal shape with amplitude of *L/1000* at midspan of the column. The columns were free to rotate about the y-axis at both ends while all other rotational degrees of freedom were

constrained. All translational movements were constrained at both ends except that the columns were free to move in the x-direction at the upper end. These boundary conditions were applied to the reference nodes of rigid surfaces forming rigid end plates (perfect load-distributing plates). All nodes of the cross sections at the upper and lower end of the columns were tied to the respective rigid surfaces; hence had to follow the movement of the reference nodes. A point load could be applied either centrically or eccentrically at the upper end of the column.

The load-carrying behavior of the composite columns in fire was numerically analyzed using three different finite element models: *model 1* considered friction between steel and concrete, and *model 2* considered perfect bonding. *Model 1* and *2* considered the influence of compatibility stresses caused by partly constrained thermal strains on the load-carrying behavior. A third model, *model 3*, considered a bonding behavior with friction equal to model 1 and did not consider thermal expansion. The interfaces between the steel and the concrete were defined by a surface-to-surface discretization. This modeling technique allowed varying the mesh density according to the geometry and the material properties assigned. It was possible to either simulate perfect bonding by tying the surfaces together or to attribute mechanical properties in the normal and the tangential direction of the interface. Both cases were implemented in two independent models: *model 1* and *3* considered friction between both materials with a friction coefficient of $\mu_f = 0.6$ and *model 2* assumed perfect bonding. The initial position of the surfaces relative to each other was adjusted to avoid overclosures due to non-matching meshes of the different parts forming the interface. The contact constraints were enforced by means of a linear penalty stiffness method in conjunction with an augmented Lagrange iteration scheme for the model without perfect bonding (*model 1*): In this case the contact state of the surfaces was first established in a Newton iteration. Secondly, the contact pressure was augmented for those nodes that were overclosed for more than a certain penetration tolerance and the contact was solved again iteratively until these overclosures were dissolved [10]. Using this advanced modeling technique the contact resolution was more precise potentially helping to obtain a converged global solution. Additionally, a more precise contact could be achieved by using an iteration which did not stop until no severe discontinuities occurred anymore to overcome convergence difficulties related, most probably, to the distribution of redundant contact pressure forces when the interface opened.

The common metal plasticity model of ABAQUS was used for the material behavior of the steel tube and the steel core. Nominal yield strengths of 235 N/mm^2 for the tube and 355 N/mm^2 for the core at ambient temperature were considered. The influence of the temperature on the constitutive behavior was considered by the stress-strain relationships according to EN 1993-1-2 [11] including strain hardening. The ABAQUS concrete damaged plasticity model was applied for the concrete as a nominal stress model (i.e. without considering material damage by specifying evolution laws for the damage variables in tension or compression). Hardening and post-failure behavior in compression were modeled according to the temperature-dependent stress-strain relationships of EN 1992-1-2 [12]. The cylinder compression strength at ambient temperature was 25 N/mm^2. The tension stiffening was accounted for by means of the fracture energy approach considering a temperature-independent value of $G_f = 0.14$ *N/mm*. ABAQUS default values of the model parameters defining the shape of the yield surface were employed and assumed also to be independent of the temperature. An angle of dilation of $\psi = 15°$ was considered. Additionally the viscoplastic regularization technique was used with $\mu = 0.1$ for the viscosity parameter to overcome convergence problems related to the constitutive equations of the concrete model and its non associated character as well as the softening in the compression zone [11]. Residual stresses of the massive steel core were considered according to the distribution proposed by [1].

Fire test data on concrete-filled steel section columns with massive core are very rare. The load-carrying tests with different load eccentricities at ambient temperature given in [1] were used for validating the numerical model. The ratio between the numerical and the experimental results for the almost centrically loaded composite columns was $P_{FEA}/P_{Exp} = 0.943$. The finite element method model presented above was found to be suitable for predicting the resistance of slender composite columns with massive steel core. Details of the validation will be given at the conference.

2.2 Calculating procedure

Composite columns in fire are subjected to both a mechanical pre-loading and a thermal action – often considered with the standard ISO time temperature curve [13]. The fire resistance time is the duration of fire exposure until column failure occurs and depends on the mechanical pre-loading and the thermal action. It was the aim of the study to determine the mechanical maximum pre-loading to reach a fire resistance of 30, 60 and 90 minutes standard ISO fire exposure. The maximum pre-loading for *model 1* and *2* (the pre-loading of *model 3* was considered equal to *model 1*) was determined iteratively since the *P–Δ* effect has a marked effect on the load-carrying capacity N_K of slender composite columns. Each iteration consisted of three calculation steps (Fig. 1): First, a static stress analysis was carried out at ambient temperature and the column was loaded successively up to the pre-loading P_0 which was estimated as a function of the column strength at ambient temperature. Secondly, the pre-calculated temperature fields (calculated in a separate and independent heat transfer analysis) were applied for consecutive time increments up to the desired fire resistance time within a static (thermal) stress analysis step. Temperature-dependent material properties for steel and concrete according to [11] and [12] including thermal expansion (for *model 1* and *2*) were considered. Finally, the column was mechanically loaded until failure occurred to determine the load reserve *ΔP* at elevated temperatures. Subsequently the pre-loading of the column had to be updated for the next iteration. The pre-loading consisted of the sum of the pre-loading and a fraction of the load reserve, both of them of the previous iteration. Considering a too large fraction of the load-reserve led to a premature failure of the column during the thermal loading since the *P-Δ* effect was more pronounced due to the higher load (Fig. 1 dashed line). The iteration process was continued until the load reserve was smaller than a limit of 2% of the sum of the pre-load of the current iteration and the load-reserve of the current iteration.

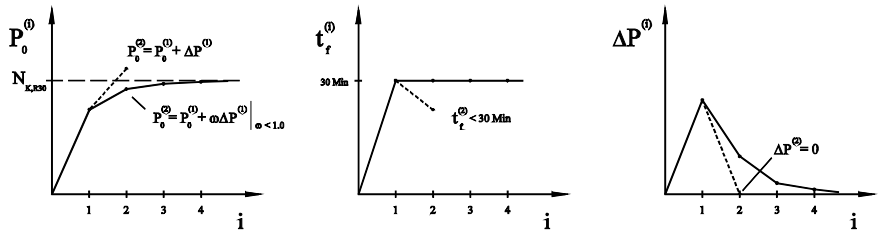

Figure 1: Iteration scheme (a) mechanical pre-loading, (b) thermal loading, (c) load reserve

3 RESULTS

3.1 Load-carrying behavior

The fundamental load-carrying behavior of concrete-filled CHS columns with massive steel core subjected to fire was numerically analyzed with the finite element model considering a frictional interface (*model 1* and *3*). The pre-loading corresponding to a given fire resistance time was determined according to the calculation procedure described in the previous section. Figure 2 (left) shows the applied axial load N_{res}, the temperature of five distinct points over the cross section θ_i (indices of the temperature refer to the position, Fig. 2 bottom right), the midspan deflection considering initial geometric imperfection $w_{tot} = w_0+w$ (indices of the displacements refer to the models used), and the end shortening u as a function of the fire exposure time t. The results are given for a composite column with an outer diameter of 273 mm and a thickness of 5 mm of the steel tube (steel grade S235), a diameter of 180 mm of the massive core (steel grade S355) and unreinforced concrete (nominal cylinder compression strength of 25 N/mm^2 at ambient temperature) as an example. A fire resistance of 30 min and an effective length of the column of 4 m were used for the calculations presented in Fig. 2.

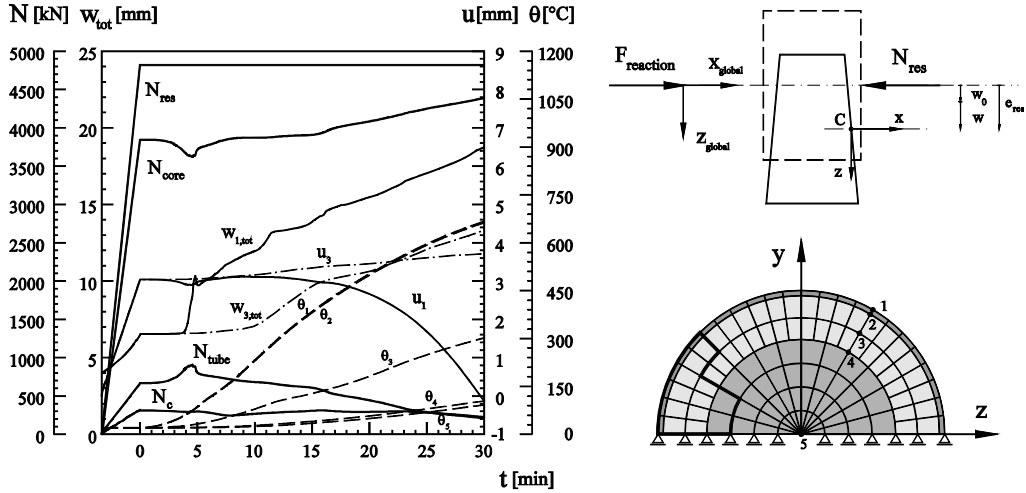

Figure 2: Axial load-time, temperature-time and deflection-time curves (left); Slice of column including axial load N, deflection w and global and local coordinates (top right) cross section with element mesh (bottom right)

Figure 2 (left) additionally shows the parts of the applied load N_{res} carried by the steel tube N_{tube}, the concrete N_c , and the steel core N_{core} in the cross section at midspan of the column. The nodal forces and the actual coordinates were used for calculating the resulting forces of every part of the cross section (tube, core and concrete) including their eccentricities relative to the centroid of the cross section. Figure 2 (top right) shows an deformed part of the column, the local coordinate system used to measure the eccentricity (without rotation for simplicity) and its relation to the global coordinate system of the model. The eccentricities e of the resulting forces of the different parts of the cross section and the corresponding moments M are given in Fig. 3 (left). Figure 3 (right) shows the averaged normal stresses in the steel core $\sigma_{i,core}$ and the steel tube $\sigma_{i,tube}$ (indices of the stresses refer to the model used) as well as stresses in the inner $\sigma_{i,inner}$ and outer parts of the concrete $\sigma_{i,outer}$. The stresses were calculated from the elements highlighted in Fig. 2 (bottom right, black line) located at midspan of the column on the compression side. Hoop compatibility compression stresses arose and enabled slightly higher stresses in the steel tube than the uniaxial yield strength.

The load-carrying behavior of concrete-filled CHS columns with steel core in fire is mainly influenced by (a) a reduction of the material properties of steel and concrete with increasing temperature, in particular a decrease of steel's stiffness and proportional limit for temperatures above 100°C and the yield strength above 400°C and (b) compatibility stresses due to partially constrained thermal strains which arose from transient temperature gradients over the cross section. The development of the midspan deflection w_{tot} during the fire exposure can be grouped into four stages (Fig. 2 left): (1) from the start of the fire exposure until approximately 4 minutes, when the deflection remained almost constant for *model 1* (with thermal expansion) and *3* (without thermal expansion); (2) from 4 to 10 minutes, when a marked increase in the deflection was observed for the model considering thermal strains (*model 1*) whereas the deflection remained almost constant for the model disregarding the thermal expansion (*model 3*); (3) from 10 to 16 minutes, when the deflection of *model 3* increased for the first time and, thus, marked the effect of the temperature-dependent reduction of the stiffness and the proportional limit, and (4) after 16 minutes, when the thermal strains had almost no influence on the midspan deflection and the curves for both models were nearly parallel.

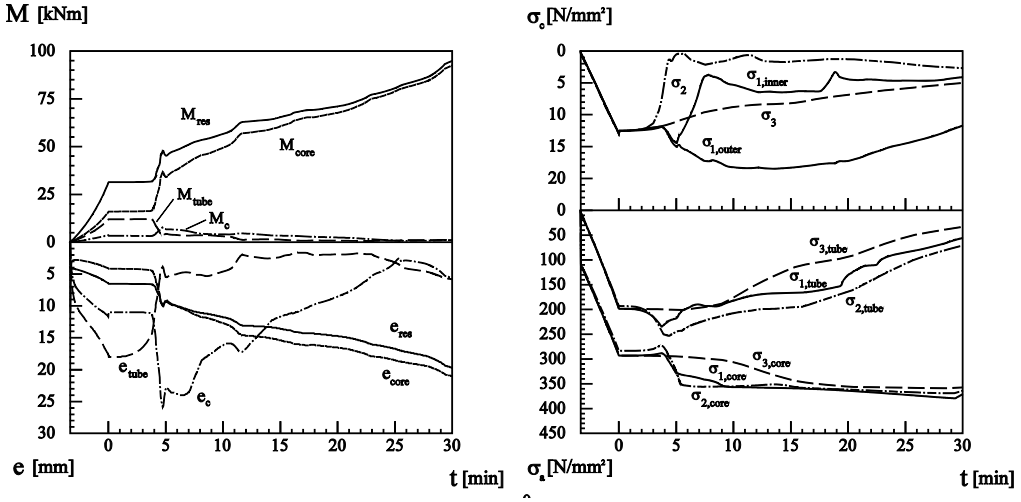

Figure 3: Bending moments (top) and eccentricities (bottom) of the different parts of the cross section at midspan (left) and stress development for the different FEM models (right) (top: concrete, bottom: steel tube and steel core).

At stage 1 the steel tube was heated up leading to thermal strains, which were constrained partially by the inner parts of the column which were still at ambient temperature. Therefore compatibility stresses arose: (a) tension stresses in the inner cooler part resulting in a marked decrease of the compression force in the steel core and in the concrete (Fig. 2 left); and (b) compression stresses in the outer part leading to an increase of the compression force in the steel tube. Using perfect bonding (*model 2*) led to higher compatibility stresses as a result of the constrained thermal strains since stress-relieving slip could not developed. These compatibility stresses led to higher compression stresses in the steel tube and a larger decrease of the concrete compression stresses (Fig. 3 right).

At the beginning of stage 2 the yield strength was reached on the compression side in the steel tube causing a localized loss of stiffness leading to a loss of bending stiffness and consequently to the increase of the deflection. The bending moment was redistributed from the steel tube to the concrete and the steel core (Fig. 3 left). The associated stress distribution of the cross section before (top) and after (bottom) the increase of the deflection is given in Figure 6 (right). The stresses of the steel tube are given in the front and the stresses of the core in the back. The concrete stresses are hidden behind the tube stresses since their magnitude is much smaller. The compression zone is located on the right side.

After approximately 10 minutes of fire exposure the end shortening of the *model 1* began to decrease and deviate from the end shortening of *model 3* (Fig. 2 left). The thermal strains now developed less constrained and the compatibility stresses less influenced the behavior of the composite column. The stresses of the inner part of the concrete started growing again (Fig. 3 right). At the beginning of stage 3 (after 10 minutes) the steel tube reached a temperature of about 200°C. The bending moment was mainly redistributed to the core.

Stage 4 was characterized by the completion of the redistribution of the moment to the steel core and the reduction of the strength of the steel tube which reached a temperature of 400°C after approximately 16 minutes. The compression force was mainly distributed to the steel core. After approximately 25 minutes the concrete reached a temperature of about 250°C and the strength decreased. The failure of the composite column was governed by a plastic failure and local buckling of the steel tube, when the core was still at a temperature of approximately 100°C.

The comparison between the results of model 1 and 3 (Fig. 2 and 3) shows the strong influence of the compatibility stresses caused by partly constrained thermal strains on the structural behavior of the composite columns during the first and second stage (start to approximately 10 minutes of fire exposure). The bonding behavior between steel and concrete mainly affects the load-carrying behavior during the second stage. Perfection bonding leads to higher compatibility stresses and higher compression stresses in the tube and a larger decrease of the concrete compression stresses (Fig. 3 right).

3.2 Parametric study

Due to large difference in calculation time and small differences in the results, in particular for the fire resistance, the simpler model considering perfect bonding (*model 2*) was used for conducting a comprehensive parametric study. The cross-sectional properties were identical to the analysis of the load-carrying behavior. The behavior of concrete-filled CHS columns with different lengths and fire exposure durations was analyzed and the results comprised the axial load N, the deflection at midspan w, and the temperature at different points of the cross section θ_i , as a function of the fire exposure time t.

Figure 4 shows the results for a column with an effective length of 4 m as an example. The pre-loading for the column with a fire resistance of 30 minutes (Fig. 4 left) was about the double of the pre-loading of the column with a fire resistance of 90 minutes (Fig. 4 right) leading to a larger midspan deflection caused by the mechanical pre-loading. The higher pre-loading also led to a larger increase of the deflection induced by the partial yielding of the steel tube. The lower pre-loading resulted in a later partial yielding of the steel tube since more compression stresses as a result of constrained thermal strains could be carried. Hence the tube had a higher temperature and exceeded 100°C when the increase of the deflection occurred which in this case was not only triggered by compatibility stresses but also by temperature-dependent stiffness reduction. The deflection at midspan after 30 and 90 minutes respectively was almost similar in magnitude (Fig. 4).

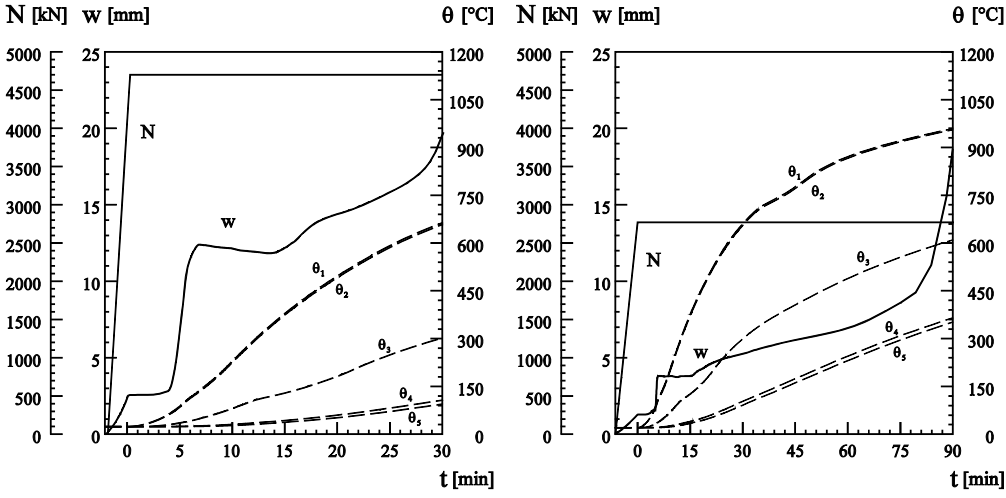

Figure 4: Axial load N, midspan deflection w and temperature θ_i of the composite column with an effective length of 4'000 mm and a fire resistance of 30 (left) and 90 minutes (right).

Figure 5 shows the results for a slender column with an effective length of 8 m as an example. It can be observed that the increase of the deflection was less abrupt compared to the shorter column of 4 m (Fig. 4). Due to the higher slenderness ratio the initial deflections caused by the pre-loading were larger than for the shorter column leading to considerable bending stresses over the cross section. Since the stresses were mainly because of bending the normal stress gradient over the cross section was steeper and

the yielding zone could not spread as quickly as for the shorter column. The end deflection of the slender columns differed markedly for the two fire resistance times (Fig. 5).

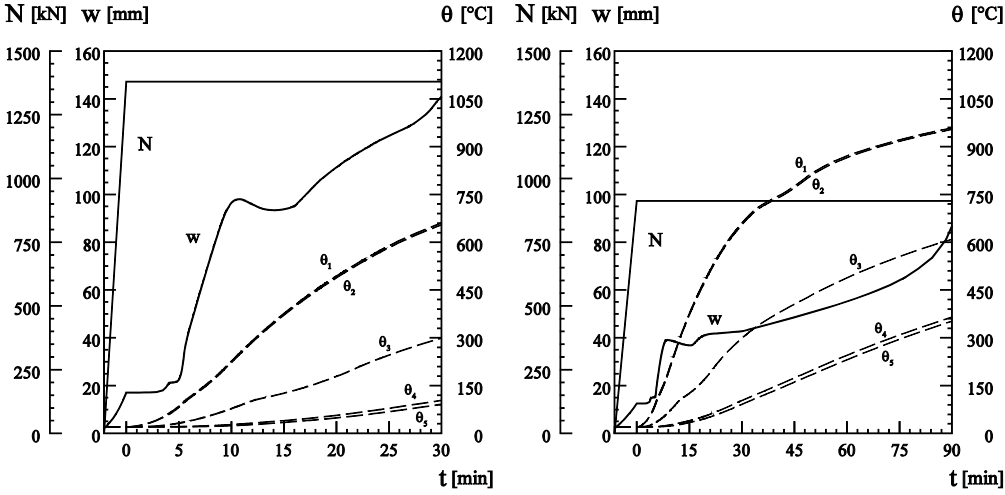

Figure 5: Axial load N, midspan deflection w and temperature θ_i of the composite column with an effective length of 8'000 mm and a fire resistance of 30 (left) and 90 minutes (right).

3.3 Buckling strength

The results of the parametric study were used to develop curves for the ultimate buckling strength. Figure 6 (left) shows the curves for ambient temperature and for fire resistance times of 30, 60 and 90 minutes. The results are given for a concrete-filled CHS column with steel core with an outer diameter of 273 mm and a thickness of 5 mm of the steel tube (steel grade S235), a diameter of 180 mm of the massive core (steel grade S355) and plain concrete (nominal cylinder compression strength of 25 N/mm^2 at ambient temperature) as an example.

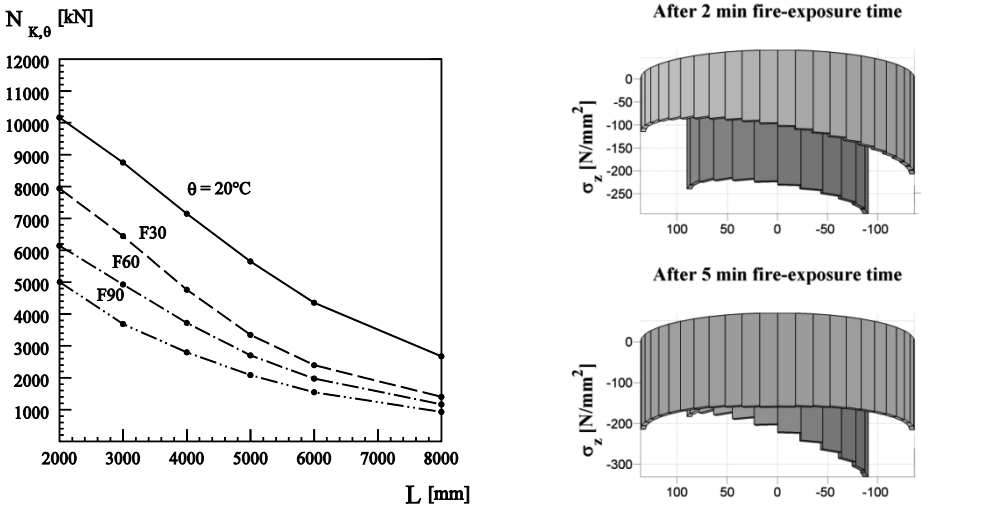

Figure 6: Curves for the buckling strength (left) and stress distributions over cross section (right).

4 CONCLUSIONS

The structural fire behavior of concrete-filled circular hollow section columns with massive steel core has been numerically analyzed. A finite element model considering temperature-dependent material properties for concrete and steel as well as the bonding behavior between steel and concrete was proposed and applied to columns with different sections and buckling lengths. Results, including temperature-, end shortening-, deflection- and stress-fire exposure time curves, have been presented. The compatibility stresses caused by partly constrained thermal strains and the bonding behavior between steel and concrete have a strong effect on the fundamental load-carrying behavior and the fire resistance of the composite columns. The results of a parametric study have been used for developing curves for the ultimate column buckling strengths for various fire resistances. The finite element model developed in this study may be used for further analyzing the fundamental structural behavior of composite columns in fire and determining their fire resistances. Further analytical and numerical studies on the fire behavior of centrically and eccentrically loaded concrete-filled CHS columns with steel core are underway and will be presented on the conference.

REFERENCES

[1] Hanswille G. and Lippes M., Einsatz von hochfesten Stählen und Betonen bei Hohlprofil-Verbundstützen, *Stahlbau*, **77**(4), 296-307, 2008.

[2] Grandjean et al., Determination de la durée au feu des profils creux remplis de béton. Rapport final, Commission des Communautés Européennes, Rechereche Technique Acier, Luxembourg, 1981.

[3] Kordina K. and Klingsch W., Fire resistance of composite columns of concrete filled hollow sections. Research report. CIDECT 15 C1/C2-83/27, Germany, 1983.

[4] Lie T.T. and Caron SE, Fire resistance of circular hollow steel columns filled with siliceous aggregate concrete. Test results, internal report no. 570, Ottawa: Institute of Research in Construction, National Research Council of Canada, 1988.

[5] Lie T.T., Chabot M. and Irwin R.J., Fire resistance of circular hollow steel sections filled with bar-reinforced concrete, Internal Report No. 636, Institute for Research in Construction, National Research Council of Canada, Ottawa 1992.

[6] Myllymäki J., Lie T.T. and Chabot M., Fire resistance tests of square hollow steel columns filled with reinforced concrete, Internal Report No. 673, Institute for Research in Construction, National Research Council of Canada, Ottawa 1994.

[7] Kodur V.K.R. and Lie T.T., Fire resistance of circular steel columns filled with fibre-reinforced concrete, ASCE, *Journal of Structural Engineering*, Vol **122**, No. 7, 776-782, 1996.

[8] Ding, J., Wang Y.C., Realistic modelling of thermal and structural behaviour of unprotected concrete filled tubular columns in fire, *Journal of Constructional Steel Research*, **64**(10), 1086-1102, 2008.

[9] Zha X.X., FE analysis of fire resistance of concrete filled CHS columns, *Journal of Constructional Steel Research*, **59**(6), 769-779, 2003.

[10] Zienkiewicz O.C. and Taylor R.L., The Finite Element Method for Solid and Structural Mechanics, Sixth Edition, Elsevier Ltd., London, 2006.

[11] EN 1993-1-2. Eurocode 3: Design of steel structures – Part 1-2: General rules – Structural fire design, Brussels, 2006.

[12] EN 1992-1-2. Eurocode 2: Design of concrete structures – Part 1-2: General rules – Structural fire design, Brussels, 2006.

[13] ISO 834. Fire-resistance tests - Elements of building construction - Part 1: General requirements, 1999.